Available online at www.sciencedirect.com
ScienceDirect
Geochimica et Cosmochimica Acta 74 (2010) 1104–1121
Geochimica et Cosmochimica Acta
www.elsevier.com/locate/gca

Slab decarbonation and CO_2 recycling in the Southwestern Colombian volcanic arc

Maria I. Marín-Cerón *, Takuya Moriguti, Akio Makishima, Eizo Nakamura

The Pheasant Memorial Laboratory for Geochemistry and Cosmochemistry, Institute for Study of the Earth's Interior, Okayama University at Misasa, Tottori-ken 682-0193, Japan

Received 6 April 2009; accepted in revised form 5 October 2009; available online 27 October 2009

Abstract

The contribution of subducted carbonate sediments to the genesis of the Southwestern Colombian arc magmas was investigated using a comprehensive petrography and geochemical analysis, including determination of major and trace element contents and Sr, Nd, Hf and Pb isotope compositions. These data have been used to constrain the depth of decarbonation in the subducted slab, indicating that the decarbonation process continues into the sub-arc region, and ultimately becomes negligible in the rear arc. We propose on the basis of multi-isotope approach and mass balance calculations, that the most important mechanism to induce the slab decarbonation is the infiltration of chemically reactive aqueous fluids from the altered oceanic crust, which decreasingly metasomatize the mantle wedge, triggering the formation of isotopically different primary magmas from the volcanic front (VF) with relatively high $^{176}Hf/^{177}Hf$, high $^{87}Sr/^{86}Sr$, negative values of εNd and lower Pb isotopes compared to the rear arc (RA).

The presence of more aqueous fluids at the volcanic front may increase the degree of decarbonation into carbonate-bearing lithologies. Moreover, with increasing pressure and temperature in the subduction system, the decrease in dehydration of the slab, leads to cessation of fluid-induced decarbonation reactions at the rear arc. This development allows the remaining carbonate materials to be recycled into the deep mantle.

1. INTRODUCTION

Decarbonation reactions at subduction zones are one of the most important processes to understand the global carbon cycle on geological time scales. However, the fate of subducted carbonate remains controversial (e.g. Kennedy and Kennedy, 1976; Yaxley and Green, 1994; Sano and Williams, 1996; Marty and Tolstikhin, 1998; Molina and Poli, 2000; Kerrick and Connolly, 2001a,b; Sato and Katsura, 2001; Snyder et al., 2001; Sadofsky and Bebout, 2003; Gorman et al., 2006; Morlidge et al., 2006). From a study of devolatization in several metasedimentary suites in fore-arc region indicates the retention of significant *C* to depths up to ~40 km in normal to cold subduction zones whereas some *C* devolatilization could occur at warm subduction zones at shallow depths (5–40 km) (Sadofsky and Bebout, 2003). This conclusion implies that the subducted slab can introduce carbonates to significant mantle depths in most subduction zones. However, King et al. (2007) suggested that melange mixing could induce decarbonation at subduction zones. Phase diagrams (e.g. Kerrick and Connolly, 2001a,b; Connolly, 2005) combined with assuming bulk compositions from the available data-set of trench subducted carbonate-bearing sediments (Plank and Langmuir, 1998) and different thermal regimens of subducted slab (Peacock and Wang, 1999), indicates that at warm subduction zones, the subducted carbonates may completely decompose in the fore-arc region so that little or no carbon is released in the volcanic arcs (Kerrick and Connolly, 2001a,b). Those authors (e.g. Kerrick and Connolly,

* Corresponding author. Present address: Universidad EAFIT, Carrera 49 # 7 Sur – 50, Medellín, Colombia, South America. Tel.: +27 57 4 2619500.
E-mail address: mmarince@eafit.edu.co (M.I. Marín-Cerón).

0016-7037/$ - see front matter © 2009 Elsevier Ltd. All rights reserved.
doi:10.1016/j.gca.2009.10.031

2001a,b; Connolly, 2005) have pointed out that unless large amount of water infiltration occurs, the batch model mechanism could be a more effective mechanism to produce slab decarbonation, but this mechanism is inadequate to explain the global CO_2 budget. Therefore, the controversy persists, if we take into account the studies of fumarolic gasses, which show that carbonate-bearing marine sediments are the main source for the CO_2 released from arc volcanism even in warm subduction zones (Marty and Tolstikhin, 1998; Sano and Williams, 1996; Snyder et al., 2001). Deep into the subduction zone system, there is a general consensus between results from high-pressure studies and metamorphic geology (e.g. Kennedy and Kennedy, 1976; Yaxley and Green, 1994; Molina and Poli, 2000; Sato and Katsura, 2001; Morlidge et al., 2006) that carbonate lithologies are stable at high pressures (>4 GPa). These observations indicate that large amount of carbonates may be introduced into the deep mantle.

To provide more evidence of the depth of decarbonation processes in natural samples, we have chosen the SW Colombian volcanic arc in order to trace the involvement of marine sediments in the arc magmas at warm subduction zones. This arc is located in the North Volcanic Zone of the Andes Cordillera, which is the result of the subduction of a young portion of Nazca Plate (~14 Ma, Hardy, 1991) beneath the North Andean Block. Geographically, this arc is located in the Eastern Tropical Pacific Ocean (ETPO, between 10° S and 20° N of latitude), where carbonates from the equatorial high productivity zone are being delivered to the subduction zone on short timescales (<15 my) and with minimal penetration of the carbon compensation depth (Edmond and Huh, 2003).

Additionally, the relatively simple geophysical structure with constant Moho depth (35–40 km) across and along the arc and small differences in the angle of subducted plate (25°–30°), with volcanoes lying at 120–200 km to the depth of Wadati-Benioff Zone (WBZ) (Fig. 1), makes this volcanic arc an ideal place to investigate the fate of carbonates sediments at subduction zones. In this study, we use comprehensive geochemical data set of four SW Colombian active volcanoes including petrography together with major and trace element compositions and Pb, Hf, Nd and Sr isotope compositions across the arc, for whole-rock samples in order to better understand decarbonation processes at subduction zones and recycling of carbon into the deep mantle.

2. GEOLOGICAL SETTING AND SAMPLES LOCATION

2.1. Regional geology

The recent volcanism in the Colombian Andes is part of the Northern Volcanic Zone, which extends 550 km long in Colombia with approximately 50 km wide (Fig. 1a), characterized by the collision of the South American, Nazca and Caribbean plates and the Panama block (Fig. 1b). Subduc-

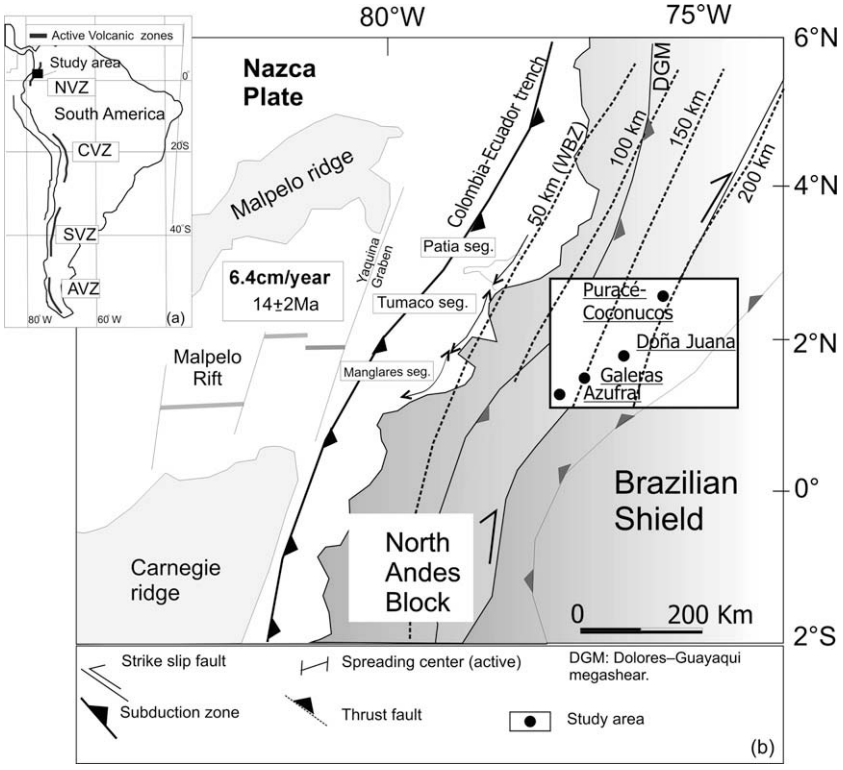

Fig. 1. (a) Volcanic zones distribution in the Andes Cordillera. (b) Tectonic setting of the NVZ in the Andes. Distribution of active volcanoes, active and inactive ridges, main fault systems and active volcanoes. Wadati-Benioff Zone (WBZ) contours represent isobaths for the top of the deep seismic zone caused by subduction of the Nazca plate beneath the North Andean Block. Solid circles indicate the studied volcanoes. (Modified from Gutscher et al., 1999; Droux and Delaloye, 1996 and references there in).

tion of the Nazca oceanic plate beneath the Andes generates the magmas that formed the volcanic complexes and Cenozoic intrusions of the Central and Western Andean Cordilleras and the Cauca-Patía graben of Colombia.

The basement of Central Andean Cordillera of Colombia is composed of Precambrian–Paleozoic metamorphic and igneous rocks (Arango and Ponce, 1982). Batholiths of granodiorite and monzonite have intruded this cordillera since the Mesozoic. In contrast the basement of the Western Andean Cordillera is mainly formed by Caribbean–Colombian oceanic plateau rocks and relicts of island arcs, which were accreted during the late Cretaceous (Kerr et al., 1996; Alvarado et al., 1997; Arculus et al., 1999; Mamberti et al., 2003). Weber et al. (2002) showed that the lower crust xenoliths beneath the SW Colombian arc have highly radiogenic in Pb isotopic composition and similar major, trace elements and Sr, Nd isotopic compositions to the oceanic basaltic rocks from the Western Cordillera.

At the Pacific offshore of Colombia, the sediment layers in DSDP/ODP site 504B and 495 showed that carbonate-rich sediments (CS) is dominant (200–325 m thickness) with a small amount of hemipelagic sediments (HS) (up to 177 m thickness) (Patiño et al, 2000; Plank et al., 2002). The carbonate-rich sediments are not pure, they also contain clay and ash layers with some metalliferous oozes near the igneous contact at DSDP/ODP site 504B (Plank and Langmuir, 1998). In this region there is a <5 km wide accretionary prism at the most southern part of the margin (see Tumaco segment, Fig. 1b), which increases up to 35 km wide to the northern part (see Patía segment, Fig. 1b). This may indicate that the sedimentary sequences deposited in this region have been almost completely subducted beneath the arc.

2.2. Sample locality and description

The recent magmatism in the Colombian Andes is mainly of explosive character with huge ignimbrite platforms, pyroclastic flows, ash fall deposits and the construction of lava dome in their submit areas. Those volcanoes exhibit systematic geochemical variation across-arc in terms of major and trace elements such as progressive increment of K_2O and Rb, with concomitant decrease in FeO and TiO_2 (e.g. Murcia and Marin, 1980; Calvache and Williams, 1997; Droux and Delaloye, 1996).

The four selected volcanoes varies with the depth to WBZ as follows: (1) Azufral volcano, located at 1°08′N–77°68′W (~140 km); (2) Galeras volcano located at 1°13′N 77°22′W (~150 km); (3) The Doña Juana Volcanic Complex located at 1°47′N 76°92′W (~170 km) and (4) Puracé–Coconucos Volcanic Complex located at 2°32′N and 76°40′W (~200 km). The samples used in this study were collected based on the volcanoes stratigraphy established by previous works (e.g. Bechon and Monsalve, 1991; Pulgarin et al., 1993; Calvache and Williams, 1997; Marin-Cerón, 2002).

Petrographic observations indicate that the SW Colombian arc in the studied area is dominantly composed of andesites with volumetrically less dacites and rhyolites

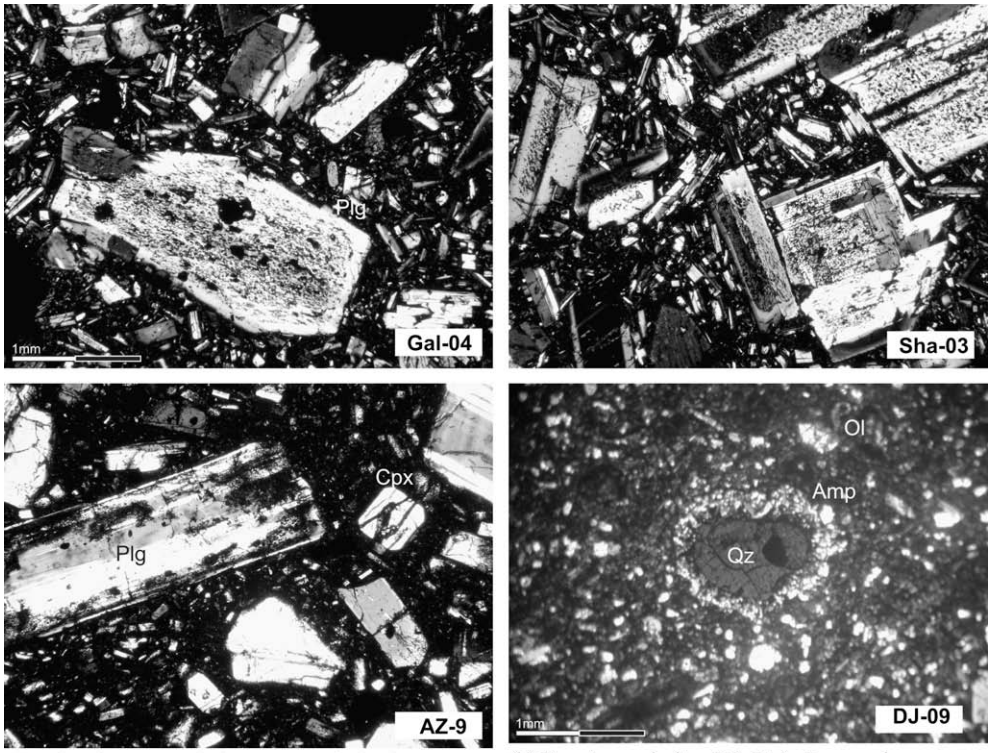

(a) Volcanic Front andesites, Az: Azufral volcano, Gal: Galeras volcano.

(b) Rear Arc andesites, DJ: Doña Juana volcano, Sha: Puracé-Coconucos volcanic complex.

Fig. 2. Thin sections of selected samples from Volcanic Front and Rear Arc Andesites.

Table 1
Major elements (wt%). trace elements (ppm) and isotopic compositions from SW Colombian volcanic arc.

Sample	Azufral volcanic complex (WBZ = 140 km)							Galeras volcanic complex (WBZ = 150 km)		
	AZ-07	AZ-08	AZ-09	AZ-10	AZ-76	AZ-205	AZ-308	GAL-1	GAL-2	GAL-4
SiO_2	58.6	57.5	57.4	74.6	61.3	66.6	59.9	57.6	60.9	58.5
TiO_2	0.80	0.70	0.70	0.10	0.74	0.40	0.80	0.80	0.70	0.80
Al_2O_3	17.2	18.2	18.3	15.3	15.6	16.1	17.4	17.6	16.8	18.0
Fe_2O_3	7.20	7.20	7.50	1.10	5.25	3.70	7.50	7.60	6.60	7.30
MnO	0.10	0.10	0.10	0.00	0.07	0.10	0.20	0.10	0.10	0.10
MgO	3.60	3.10	3.30	0.20	3.23	1.20	3.20	3.70	3.10	3.50
CaO	6.70	5.50	6.70	1.80	5.02	3.90	6.60	7.10	5.90	6.50
Na_2O	3.60	3.30	3.70	4.30	3.77	4.00	3.50	3.60	3.80	3.70
K_2O	1.30	1.30	1.20	2.70	2.32	1.80	1.30	1.40	2.00	1.70
P_2O_5	0.20	0.20	0.20	0.00	0.20	0.10	0.20	0.20	0.20	0.20
LOI	0.90	2.40	1.20	0.10	2.16	1.60	0.10	0.40	0.20	0.30
SUM	100.2	99.5	100.3	100.2	99.7	99.5	100.7	100.1	100.3	100.6
Ppm										
Cr (XRF)	48.3	51.7	31.1	n.d	92.0	12.0	39.8	39.2	24.8	23.3
Ni (XRF)	25.2	22.8	14.8	n.d	42.9	1.73	27.1	19.3	16.6	16.4
Li	11.3	18.3	10.7	21.9	17.9	32.3	11.4	13.5	16.8	15.7
Be	0.74	0.89	0.76	1.25	1.33	1.00	0.77	0.80	0.93	0.93
Rb	28.1	29.1	26.9	86.8	77.5	45.2	30.3	37.3	56.3	42.8
Sr	488	429	518	403	506	487	506	520	459	523
Y	17.9	19.7	14.9	4.0	18.0	10.0	20.2	18.0	19.9	18.9
Cs	0.49	0.91	0.80	3.28	2.59	2.04	0.55	1.64	2.54	1.94
Ba	737	811	671	1945	977	1047	742	692	827	748
La	12.1	13.5	9.4	15.2	25.7	13.4	12.6	14.6	18.5	16.7
Ce	25.1	28.3	19.3	29.7	51.3	26.1	26.1	30.4	38.6	34.2
Pr	3.36	3.87	2.57	3.68	6.33	3.29	3.57	3.87	4.83	4.38
Nd	14.8	17.0	11.1	14.2	25.1	13.3	15.4	16.5	20.2	18.4
Sm	3.40	3.92	2.58	2.45	4.82	2.67	3.52	3.54	4.18	4.23
Eu	1.04	1.19	0.97	0.65	1.15	0.81	1.07	1.00	1.05	1.06
Gd	3.27	3.73	2.46	1.78	3.92	2.18	3.44	3.27	3.68	3.58
Tb	0.51	0.59	0.40	0.20	0.57	0.31	0.54	0.50	0.57	0.54
Dy	2.99	3.33	2.44	0.92	2.99	1.62	3.21	2.94	3.24	3.06
Ho	0.63	0.67	0.52	0.16	0.58	0.32	0.67	0.62	0.67	0.64
Er	1.63	1.69	1.37	0.36	1.45	0.78	1.73	1.62	1.76	1.66
Tm	0.25	0.25	0.23	0.05	0.22	0.11	0.26	0.25	0.27	0.25
Yb	1.75	1.77	1.57	0.36	1.44	0.78	1.81	1.70	1.85	1.76
Lu	0.25	0.25	0.23	0.05	0.20	0.11	0.26	0.25	0.27	0.25
Pb	4.18	5.33	5.22	12.55	11.59	8.12	4.37	8.45	10.91	9.26
Th	2.75	2.53	2.40	3.75	10.27	3.27	2.84	5.14	7.77	5.94
U	1.28	1.15	1.11	2.20	3.59	1.84	1.33	2.12	3.24	2.46
B	18.4	7.0	7.2	11.8	21.7	10.6	7.4	13.9	21.8	17.0
Zr	123	86	90	55	188	42	97	115.0	152.2	133.3
Hf	3.51	2.48	2.42	1.95	4.87	1.43	2.63	3.1	4.1	3.6

(*continued on next page*)

Table 1 (*continued*)

Sample	Azufral volcanic complex (WBZ = 140 km)							Galeras volcanic complex (WBZ = 150 km)		
	AZ-07	AZ-08	AZ-09	AZ-10	AZ-76	AZ-205	AZ-308	GAL-1	GAL-2	GAL-4
Nb	9.67	3.50	3.71	2.56	7.38	3.84	3.61	3.9	5.3	4.7
Ta	0.66	0.23	0.24	0.23	0.49	0.30	0.24	0.3	0.4	0.3
$^{206}Pb/^{204}Pb$	18.99	19.00	18.94	18.99	19.09	19.01	18.99	19.06	19.06	19.05
$^{207}Pb/^{204}Pb$	15.64	15.64	15.61	15.63	15.66	15.64	15.64	15.66	15.66	15.66
$^{208}Pb/^{204}Pb$	38.75	38.77	38.69	38.74	38.89	38.77	38.75	38.86	38.86	38.85
$^{87}Sr/^{86}Sr$	0.704196 ± 8	0.704220 ± 8	0.704167 ± 9	0.704256 ± 7	0.704354 ± 7	0.704203 ± 9	0.704199 ± 9	0.704223 ± 9	0.704208 ± 9	0.704178 ± 9
$^{143}Nd/^{144}Nd$	0.512884 ± 4	0.512877 ± 4	0.512913 ± 5	0.512850 ± 5	0.512767 ± 5	0.512886 ± 10	0.512871 ± 4	0.512872 ± 4	0.512858 ± 5	0,704178 ± 9
εNd	4.61**	4.49**	5.36*	3.95**	2.51	4.83*	4.55*	4.38**	4.10**	4.26**
$^{176}Hf/^{177}Hf$	0.283054 ± 2	0.283050 ± 2	0.283066 ± 2	0.283040 ± 2	0.283048 ± 2	0.283051 ± 1	0.283048 ± 2	0.283035 ± 2	0.283029 ± 2	0.283040 ± 2
εHf	10.0	9.8	10.4	9.5	9.8	9.9	9.8	9.3	9.1	10.0

Sample	Doña Juana volcanic complex (WBZ = 170 km)						Purace-Coconucos volcanic complex (WBZ = 190 km)				
	DJ-01	DJ-09	DJ-10	DJ-11	DJ-12	DJ-14	PPU-01	SHA-03	T-01	T-03	T-05
SiO_2	64.0	53.0	57.5	62.4	65.2	60.6	59.8	60.5	62.6	58.0	58.4
TiO_2	0.70	1.30	0.90	0.70	0.80	0.80	0.80	0.80	0.70	0.90	0.80
Al_2O_3	16.6	13.7	16.0	16.8	16.4	16.7	16.5	16.1	14.9	16.8	16.9
Fe_2O_3	5.10	8.10	8.10	5.40	5.50	6.30	6.40	6.50	6.20	7.00	7.70
MnO	0.10	0.10	0.10	0.10	0.10	0.10	0.10	0.10	0.10	0.10	0.10
MgO	1.90	6.20	5.20	2.10	2.10	3.10	3.30	4.10	2.70	3.40	3.30
CaO	4.50	8.90	8.00	4.60	4.20	5.10	5.50	6.40	4.20	6.10	6.30
Na_2O	4.40	3.20	3.10	4.30	4.30	3.90	3.90	3.80	3.80	3.70	3.50
K_2O	2.20	2.00	1.10	2.60	2.10	1.70	2.40	2.10	3.50	2.30	1.70
P_2O_5	0.20	0.50	0.20	0.20	0.20	0.30	0.30	0.20	0.20	0.30	0.20
LOI	0.50	2.30	0.00	0.90	0.00	1.70	1.10	0.20	0.70	1.00	1.00
SUM	100.2	99.3	100.2	100.1	100.9	100.3	100.1	100.8	99.6	99.6	99.9
Cr (XRF)	19.7	327.9	159.4	17.4	19.2	73.9	75.9	29.3	23.5	32.4	21.9
Ni (XRF)	5.5	120.1	9.9	6.6	6.2	22.4	20.3	19.0	15.9	19.7	9.1
Li	24.3	12.2	7.6	10.3	10.3	22.2	17.2	16.0	24.8	16.3	11.2
Be	1.37	1.44	0.86	1.65	1.36	1.20	1.33	1.21	1.54	1.24	1.09
Rb	65.1	52.5	29.9	68.6	27.9	41.6	72.2	67.3	134.4	66.9	53.4
Sr	447	791	455	594	775	479	729	717	540	734	615
Y	13.7	20.0	23.9	14.4	25.7	15.2	15.8	17.1	20.2	18.9	20.4
Cs	2.80	2.12	0.73	1.23	0.75	3.10	1.64	2.28	5.51	2.87	1.05
Ba	1111	1190	609	1176	1059	931	1092	997	1197	1030	827
La	21.2	38.2	15.0	31.3	42.3	19.2	24.4	20.7	28.7	23.8	18.7
Ce	42.8	74.6	30.0	52.4	68.6	37.7	47.4	42.0	56.2	47.7	38.3
Pr	5.23	8.68	3.88	7.24	10.91	5.16	5.73	5.02	6.36	5.86	4.79
Nd	21.1	34.7	16.6	28.3	46.9	21.8	22.7	20.0	24.1	23.3	19.6
Sm	4.16	6.29	3.71	5.05	8.90	4.45	4.28	3.90	4.64	4.68	4.21
Eu	1.13	1.85	1.13	1.47	3.22	1.30	1.20	1.06	1.01	1.23	1.19
Gd	3.43	5.13	3.76	3.81	7.49	3.74	3.63	3.39	3.78	3.98	3.60
Tb	0.48	0.69	0.61	0.51	0.95	0.53	0.51	0.50	0.56	0.56	0.55
Dy	2.40	3.60	3.77	2.62	4.47	2.71	2.78	2.83	3.16	3.15	3.24

Ho	0.44	0.67	0.81	0.48	0.78	0.50	0.55	0.57	0.64	0.63	0.69	
Er	1.07	1.63	2.15	1.14	1.70	1.21	1.38	1.49	1.70	1.60	1.81	
Tm	0.16	0.23	0.34	0.17	0.22	0.17	0.21	0.23	0.27	0.24	0.28	
Yb	1.05	1.54	2.34	1.08	1.33	1.17	1.43	1.60	1.86	1.67	1.97	
Lu	0.15	0.21	0.34	0.15	0.18	0.16	0.20	0.23	0.27	0.24	0.29	
Pb	12.76	10.77	6.86	11.56	9.55	10.54	8.76	10.05	14.53	10.49	11.74	
Th	8.39	8.16	4.74	9.75	3.41	6.52	10.85	9.44	18.06	10.45	6.56	
U	3.80	2.89	1.76	2.56	1.06	2.67	3.77	3.61	8.27	4.10	2.40	
B	19.0	8.6	6.1	5.9	6.6	9.3	21.9	13.5	38.1	10.2	9.1	
Zr	57	155	74	156	166	78	79.1	139.8	117	109	113.0	
Hf	2.20	3.80	2.20	4.00	4.20	2.40	2.4	3.7	3.95	3.12	3.0	
Nb	4.60	28.60	4.10	5.70	7.90	6.00	8.3	7.7	6.03	10.57	6.0	
Ta	0.50	1.60	0.30	0.30	0.40	0.40	0.6	0.5	0.51	0.71	0.4	
$^{206}Pb/^{204}Pb$	19.05	19.05	19.12	19.03	18.99	19.06	18.93	18.89	18.93	18.92	19.04	
$^{207}Pb/^{204}Pb$	15.67	15.66	15.68	15.66	15.65	15.67	15.65	15.64	15.64	15.64	15.69	
$^{208}Pb/^{204}Pb$	38.88	38.87	38.94	38.85	38.80	38.89	38.80	38.74	38.77	38.75	38.94	
$^{87}Sr/^{86}Sr$	0.704461 ± 10	0.704295 ± 10	0.704090 ± 10	0.704296 ± 8	0.704225 ± 8	0.704400 ± 9	0.704352 ± 10	0.704179 ± 9	0.704214 ± 10	0.704200 ± 9	0.704192 ± 10	
$^{143}Nd/^{144}Nd$	0.512808 ± 5	0.512870 ± 5	0.512798 ± 5	0.5128387 ± 5	0.512846 ± 3	0.512828 ± 7	0.512806 ± 2	0.512807 ± 5	0.512823 ± 6	0.512823 ± 4	0.512807 ± 4	
εNd	3.12	4.33	2.93	3.73	3.87	3.52	3.08	3.12	3.43	3.43	3.45	
$^{176}Hf/^{177}Hf$	0.282987 ± 2	0.282943 ± 4	0.282961 ± 3	0.282985 ± 3	0.282979 ± 4	0.282994 ± 3	0.282958 ± 3	0.282966 ± 2	0.282977 ± 2	0.282977 ± 2	0.282982 ± 2	
εHf	7.59	6.07	6.68	7.53	7.31	7.86	6.57	6.86	7.26	7.26	7.43	

εNd values were calculated using CHUR of $^{143}Nd/^{144}Nd = 0.512638$ after normalization by la Jolla Nd = 0.511869* and La Jolla Nd = 0.511878**. The correction factor between PML Nd and La Jolla was 1.000266. For Sr, Nd, Hf isotopes, the 2s mean are not shown in the table.

(Calvache and Williams, 1997; Droux and Delaloye, 1996). Phenocrysts of plagioclase, orthopyroxene, clinopyroxene and hornblende are the major crystal components; titanomagnetite, ilmenite and apatite are always present as minor phases, similar to the petrography reported elsewhere (e.g. Calvache and Williams, 1997; Droux and Delaloye, 1996).

The andesites and dacites of Southwestern Colombian volcanoes are generally porphyritic (modal phenocryst up to 50%, Fig. 2a and b). The andesites group from the Volcanic Front (VF, formed by Azufral and Galeras volcanoes) and the Rear Arc (RA, formed by Doña Juana and Puracé–Coconucos volcanic complexes) are petrographically similar, with some mineralogical differences related to the higher modal abundances of Ca-rich pyroxenes, small amounts of amphibole (~1%) and the absence of olivine and quartz at the VF compared to the RA (see Fig. 2a and b).

In general, the analyzed samples exhibit several disequilibrium features such as reverse and complex zoning profiles in plagioclase and pyroxenes; sieve textures in plagioclase; the ubiquity of amphibole phenocrysts with reaction rims or completely replaced by oxides; and presence of melt inclusions in plagioclase. Corona reactions rims are usually found around quartz in the presence of olivine in the RA andesites (see Fig. 2b.).

Existing petrographic information (e.g. Calvache and Williams, 1997; Droux and Delaloye, 1996; and the present study) indicates that the andesites at the study area cannot be derived only by fractional crystallization of mantle-derived basalts, and therefore, the several disequilibrium features above mentioned and the lack of basalts may suggest assimilation and/or magma mixing process of crustal materials by mantle-derived arc-magmas, as will be discussed in the following sections.

3. ANALYTICAL METHODS

Samples for this study are basaltic andesites, andesites, dacites and rhyolites from four Plio-Quaternary Colombian volcanoes: Azufral, Galeras, Doña Juana and Puracé–Coconucos volcanic complexes. All analyses were carried out at the Pheasant Memorial Laboratory (PML) of the Institute for Study of the Earth's Interior (ISEI) at Misasa (Nakamura et al, 2003). Rock specimens were crushed by a jaw crusher to coarse chips 3–5 mm in diameter. The chips were rinsed with deionized water in an ultrasonic bath at least three times, and then dried at 100 °C for 12 h. The washed chips were ground using an alumina puck mill.

Major element compositions, including Cr and Ni, were determined by XRF (Phillips PW2400) using glass beads made by mixing 500 mg of powdered sample and 5 g of lithium tetraborate as a flux (Takei, 2002). Loss on ignition (L.O.I.) was determined gravimetrically. Typical analytical errors in SiO_2, Na_2O, K_2O, Cr and Ni were less than 0.06%, 0.3%, 0.7%, 2% and 3%, respectively (Takei, 2002). The difference in duplicate analysis of L.O.I. was generally less than 0.1%. In this study, the quality of the major element analyses assessed by totals is 100 ± 0.8%.

Trace element concentrations were measured by Quadrupole Inductively Coupled Plasma Mass Spectrometer

(Q-ICP-MS) using an Agilent 7500cs system, following the procedures of Makishima and Nakamura (2006) for REEs, Li, Be, Rb, Sr, Y, Cs, Ba, Pb, Th and U, and of Lu et al. (2007) for B, Zr, Nb, Hf and Ta. The analytical reproducibility (RSD%) of ICP-MS data was less than 5%. The Teflon® bomb decomposition method (4 days at 245 °C) was used for samples containing acid-resistant minerals such as zircon (Makishima et al., 1999). To the silica-rich samples such as dacites and rhyolites, magnesium was added in order to suppress AlF_3 formation during the acid digestion processes at 245 °C using Teflon® bomb (Takei et al., 2001). All major and trace elements analyses were run in duplicated sample.

Isotope analyses of Sr, Nd and Pb were performed using TIMS (Finnigan MAT261, MAT262 and Triton TI) in static multicollection mode following the methods described in Yoshikawa and Nakamura (1993), Nakamura et al. (2003) and Kuritani and Nakamura (2003) for Sr, Nd and Pb isotope analyses, respectively. The determination of Hf isotope ratios was undertaken using MC-ICP-MS (Finnigan, Neptune), following Lu et al. (2007). Isotope fractionation of Sr, Nd and Hf during the analyses was corrected using $^{86}Sr/^{88}Sr = 0.1194$, $^{146}Nd/^{144}Nd = 0.7219$ and $^{179}Hf/^{177}Hf = 0.7325$ as normalization factors.

Measured ratios of standard materials were $^{87}Sr/^{86}Sr = 0.710246 \pm 6$ (2σ) for NBS987 ($n = 15$) and $^{206}Pb/^{204}Pb = 16.942 \pm 16$ (2σ),$^{207}Pb/^{204}Pb = 15.500 \pm 16$ (2σ), $^{208}Pb/^{204}Pb = 36.727 \pm 42$ (2σ) for NIST981 ($n = 16$), 143Nd/144Nd $= 0.511732 \pm 3^{*}$(2σ, $n = 10$; measured by MAT262) and 143Nd/144Nd $= 0.511741 \pm 14^{**}$ (2σ, $n = 10$; measured by Triton TI) for in-house standard, PML Nd, which corresponds to $^{143}Nd/^{144}Nd = 0.511860$ of La Jolla. In Table 1, $^{143}Nd/^{144}Nd$ ratios obtained by TIMS without correction were shown and εNd values were calculated using CHUR of $^{143}Nd/^{144}Nd = 0.512638$ after normalization by La Jolla Nd $= 0.511869^{*}$ and La Jolla Nd $= 0.511878^{**}$ for the samples measured by MAT 262 and TRITON TI, respectively (see Table 1): the correction factor between

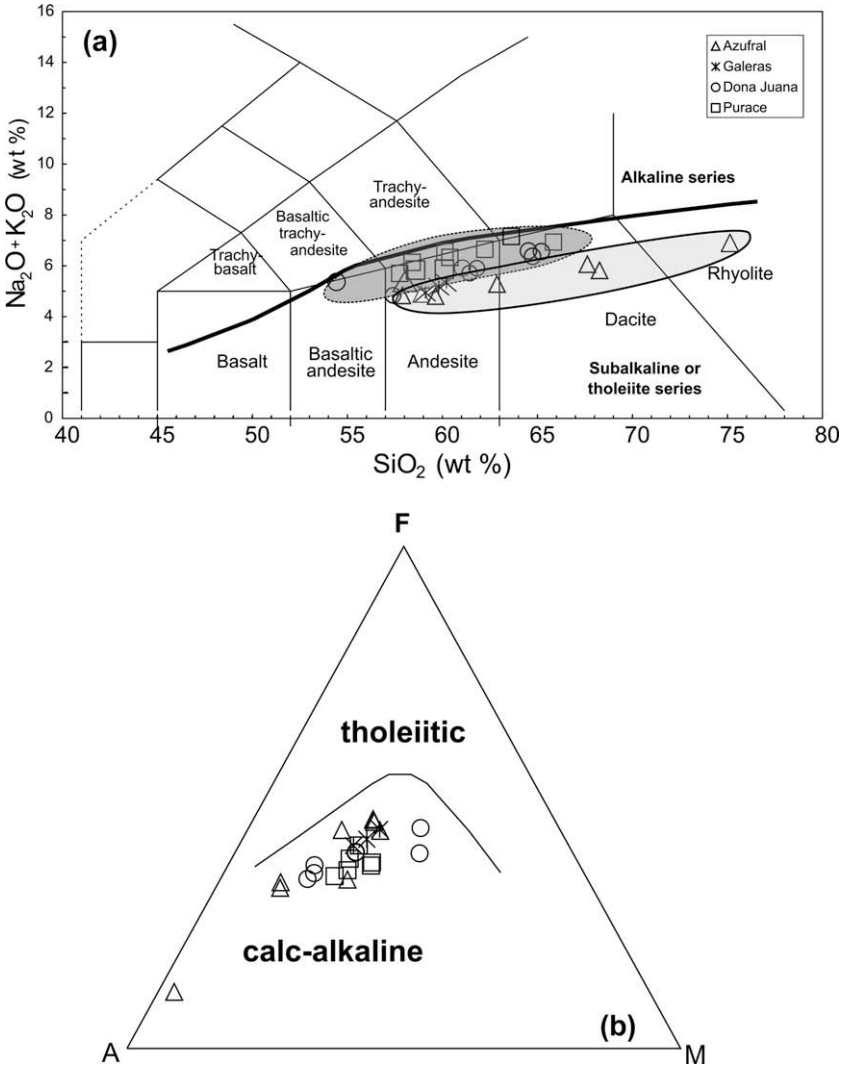

Fig. 3. (a) Total alkalis vs silica diagram of lavas from the volcanic front and the rear-arc volcanoes of the SW Colombian volcanic arc. Boundaries in the total alkalis are from LeMaitre et al. (1989) (b) AFM diagram for SW Colombian volcanic arc.

PML Nd and La Jolla was 1.000266 (Makishima et al., 2008).

The reproducibility of Hf isotope analysis using in-house standard, JMC14374 (see Lu et al., 2007), and reference rock sample, GSJ JB-3, were 0.282187 ± 8 (2σ, $n = 24$) and 0.283227 ± 3 (2σ, $n = 4$) in $^{176}Hf/^{177}Hf$ isotope ratio, respectively. εHf values were calculated using $^{176}Hf/^{177}Hf_{\_CHUR} = 0.282772$. All $^{176}Hf/^{177}Hf$ ratios in Table 1 were normalized to JMC14374 = 0.282192, which corresponds to JMC475 = 0.282160. Total procedural blanks for Sr, Nd, Pb and Hf were less than 70, 7, 10 and 5 pg, respectively, and negligible in this study.

4. RESULTS

4.1. Major and trace elements

The SW Colombian volcanic arc shows a remarkable across-arc variation of K_2O. Based on the total alkalis–silica (TAS) classification (LeMaitre et al., 1989), all samples fall in the field of basaltic andesite – andesite – dacite-rhyolite (Fig. 3a). Total alkalis contents also differ systematically between the volcanic front (VF) and the rear arc (RA). Volcanic front and the rear arc lavas plot in the calc-alkaline suite showing iron enrichment features in the FeO^*/MgO in the AFM diagram (Fig. 3b). The volcanic front lavas plot in the medium-K field and the rear-arc lavas at the limit of the medium-K to the high-K; this across arc variation is a general characteristic of volcanic rocks in subduction zones worldwide (e.g. Gill, 1981). The MgO, TiO_2, Al_2O_3 and P_2O_5 contents (see Table 1) show no systematic differences between the VF and the RA lavas at a given SiO_2 content. In general, each volcanic center defines linear chemical trend in contrast with to the curved trends diagnostic of fractional crystallization alone.

Primitive mantle normalized trace-element patterns for SW Colombian lavas are shown in Fig. 4a. The lavas display a typical volcanic arc characteristic including positive anomalies of fluid mobile elements, B, Pb, Sr and Li and negative anomalies in the high field strength elements (HFSE). The chondrite-normalized rare element diagram (Fig. 4b) shows a clear distinction between the VF and the RA samples, which could be interpreted as the effect of different degree of partial melting, with the smaller melt fraction at the RA producing enrichment in the light rare

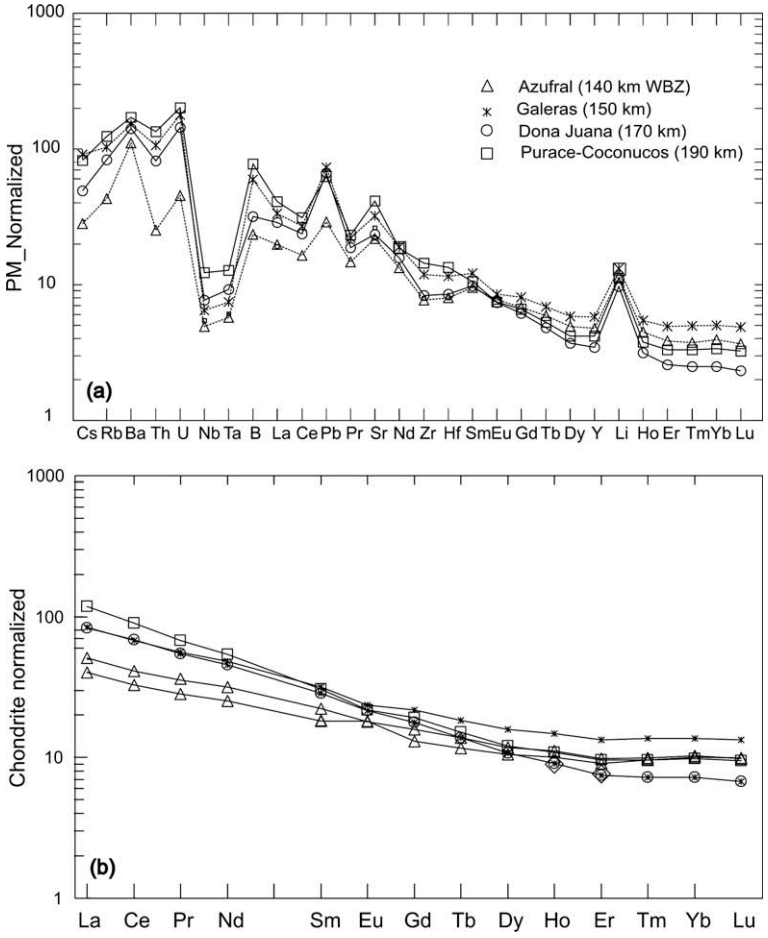

Fig. 4. (a) Primitive mantle normalized trace element diagram for SW Colombian volcanoes for selected samples ($SiO_2 \sim 57$–58%). Normalizing values from McDonough and Sun (1995). (b) Chondrite normalized REE diagram (Normalizing values from McDonough and Sun (1995).

elements (LREE). Trace element ratios such as Ba/Nb and Ba/Th, show a clear across arc variation, which is higher at the volcanic front compared to the rear arc (Fig. 5), such variation are consistent with those observed in the Central America volcanic arc (Patiño et al., 2000). On the other hand, Pb/Ce shows weak variation and B/Nb does not show any systematic variation across-arc; both trace element ratios generally decrease with WBZ as have been well documented in basaltic lavas in other volcanic arcs such as Izu, Kurile, Kamchatka and northeastern Japan arcs (e.g. Ishikawa and Nakamura, 1994; Ishikawa and Tera, 1997; Ishikawa et al., 2001; Hochstaedter et al., 2001; Moriguti et al., 2004a,b). Large crustal assimilation and/or fractional crystallization in the SW Colombian arc may obscure the across arc variation of those abundance ratios observed clearly in other arcs.

All of the samples analyzed, independent of their silica content show fluid-mediated trace element signature (Fig. 4a) and moreover, there is not any evidence of adakite-like magma signature (such as strong fractionation of heavy rare earth elements (HREE), absence of Eu anomalies, high Sr/Y and Zr/Sm and low Nb/Ta ratios, e.g. Defant and Drummond, 1990), suggested in warm subduction zones.

4.2. Pb, Nd, Hf and Sr isotopic systematics

The isotope data of andesite, dacite and rhyolites of all the volcanoes studied are summarized in the Table 1. The whole volcanic suite shows $^{87}Sr/^{86}Sr$ ratios (0.704167–0.704461) and $^{143}Nd/^{144}Nd$ ratio (0.512798–0.512913), which are similar to the values for the North Andean Volcanic Zone (Wilson, 1989 and reference there in). These values contrast with the Central Volcanic Zone of the Andes Cordillera, where the variations of $^{87}Sr/^{86}Sr$ (0.7056–0.7149) and $^{143}Nd/^{144}Nd$ (0.5121–0.5124) have been related to the extensive modification of the mantle-derived magmas as they ascend through an exceptionally thick crust (e.g. Hildreth and Moorbath, 1988; Hawkesworth and Clarke, 1994).

The most notable isotopic signature is the Pb isotope enrichment, which is the most radiogenic among all the Andean volcanic zones (Harmon et al., 1984, Wilson, 1989 and reference there in), and they plot in the lower crustal region (Fig. 6a). The εHf values of Andean cordillera volcanic zones range from 6 to 10, which are similar to the lower crust xenoliths values measured in the present study ($\varepsilon Hf = 8.99$, $^{176}Hf/^{177}Hf = 0.283026$, see Fig. 6b and Table 2). The whole volcanic suite correlates well with the lower crust composition in terms of all isotopes (Fig. 6a and b).

There is no basalts across the arc; nevertheless, the SW Colombian lavas do not show differences in the isotopic compositions of lavas from an individual volcano over the silica compositional range. Therefore, despite the complexity noted above, the volcanic front (Azufral volcanic complex, WBZ = 140 km) and rear arc (Puracé–Coconucos volcanic complex, WBZ = 200 km) volcanoes, show a clear variation in terms of K and total alkalis elements, which also present distinct trends in terms of Pb, Hf–Nd and Hf–Pb isotopic systematics (Fig. 7a and b). The volcanoes located in between 140 and 170 km to WBZ (Galeras and Doña Juana volcanoes) show similar and transitional signatures.

5. DISCUSSION

5.1. Determination of the end-member components

It is often suggested that the Andean magmatism was initiated by the dehydration of the subducted oceanic lithosphere (e.g. Thorpe, 1984) resulting in the addition of subducted components into and melting of the overlying mantle wedge. This conclusion is derived from one characteristics feature, which appears to be common to subduction-related magmatism such as positive anomalies of the fluid-mobile elements B, Pb, Sr and Li and depletion of fluid-immobile elements such as Nb and Ta. This is indicative of a component released from the subducted slab and

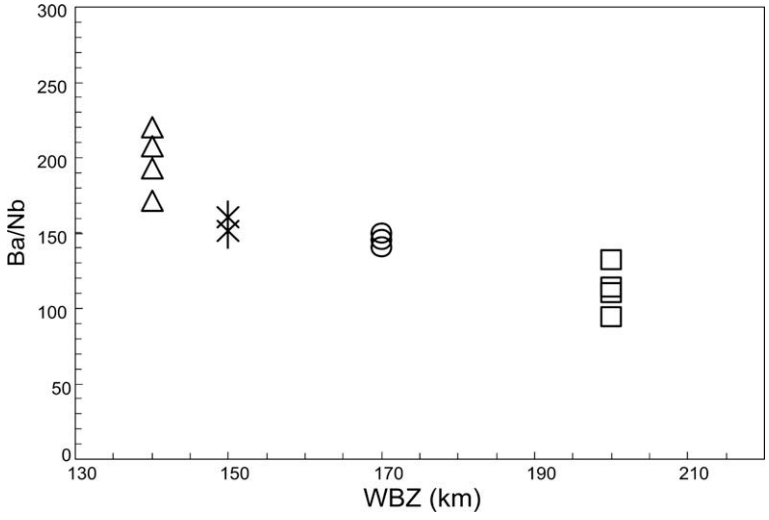

Fig. 5. Ba/Nb variation across-arc for the SW Colombian volcanic arc.

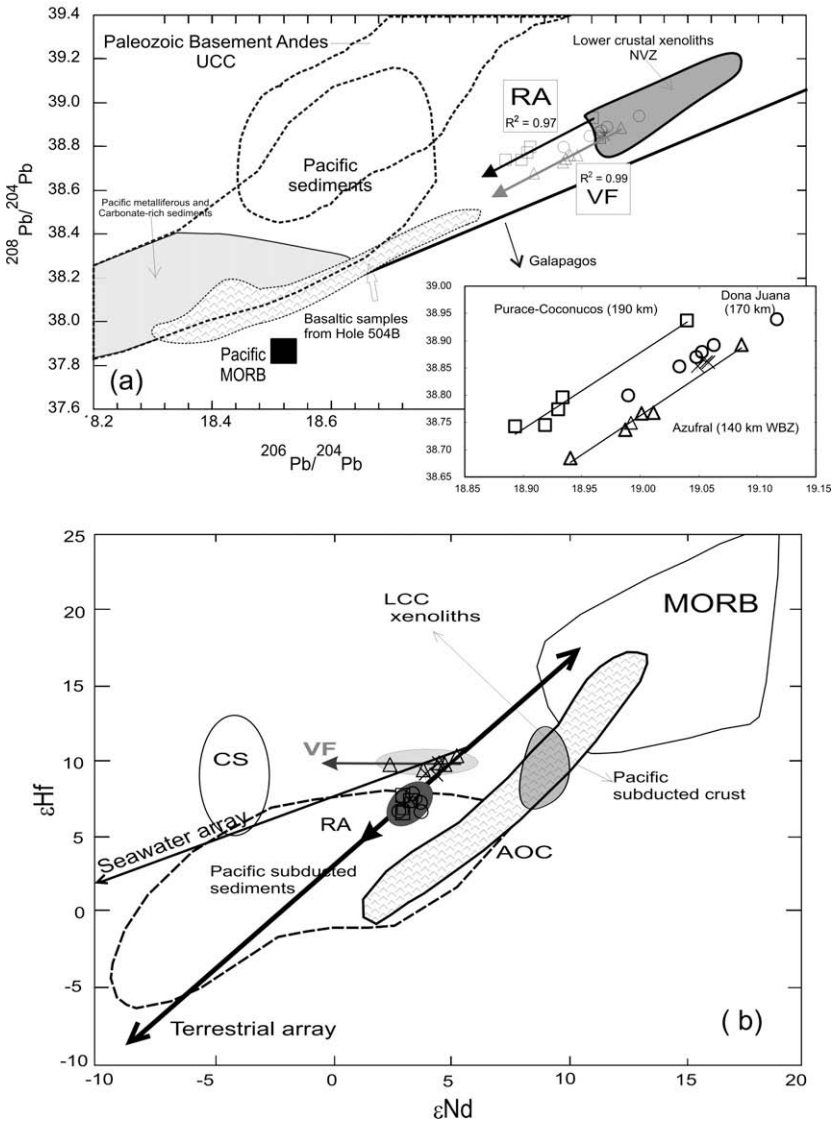

Fig. 6. (a) Lead isotopic systematics of the SW Colombian volcanic arc including the identification of possible end-members involved in the generation of andesite rocks. The squares represent assumed values for CS (Carbonate-rich Sediments); HS (Hemipelagic sediments); AOC (average Altered Oceanic Crust, hole 504b); Pacific MORB (e.g. White et al., 1987); LCC (Lower Continental Crust xenoliths, Weber et al., 2002). Pacific Sediments field (Dasch, 1981; White et al., 1986); AOC (Pedersen and Furnes, 2001); DSDP/ODP Hole 504; UCC (Chiaradia and Fontbote, 2002); Metalliferous sediments form DSDP leg 92 (Barret et al., 1987); Caribean-Colombian Oceanic Plateau (Thompson et al., 2004). The inset figure shows a clear bimodal mixing trend between lower crustal materials and primary magma for each volcano in the Southwestern Colombian arc. (b) εHf–εNd diagram for SW Colombian volcanic arc. The VF volcanoes are showing almost horizontal variation pointing out the influence of CS, which plot close to the seawater array. A different trend is shown by RA volcanoes, which plot on the mantle-terrestrial array indicating a weak or negligible influence of CS. OIB, Pacific subducted crust and Pacific subducted sediments fields are from Pearce et al. (1999) and Nowell et al. (1998). End members are the same as Pb isotopic systematics. Hf isotopes composition of LCC from the present study and Nd isotopes from Weber et al. (2002). MORB and depleted island arcs are from Marini et al. (2005) and reference there in.

consistent with the general features of trace elements in slab-derived fluid related arc volcanics (e.g. Perfit et al., 1979; Nakamura et al., 1985; Sakuyama and Nesbrit, 1986; Ryan and Langmuir, 1987; Morris and Tera, 1989). This trace element signature is interpreted to be produced by fluids released from the subducted slab. The absence of adakaite-like signature described before, implies that the thermal conditions beneath the SW Colombian arc did not reach the temperatures required for melting of this young (~14 Ma, Hardy, 1991) and, therefore, warm subducted slab, so that dehydration processes could be induced and play an important role in the formation of magmas in Colombian arc. However, taking into account that the primary signatures of those andesitic rocks may be obscured by the significant crustal involvement, we propose a multi-isotopic approach to trace the involvement of subducted

components: Altered Oceanic Crust (AOC), subducted sediments: Hemipelagic Sediments (HS) and Carbonate-rich Sediments (CS).

The clear linear compositional variations in Pb isotope systematics (Fig. 7a) indicate that the magma of each volcanic center was formed by mixing of two homogeneous end-member components: lower crust and primary subducted-related magma. The variation in the isotopic composition of the primary magmas seen in Fig. 7, may indicate involvement of different subduction component added to the mantle derived magmas from volcanic front to the rear arc volcanoes.

In general, three end-member components, mantle wedge, altered oceanic crust (AOC) and hemipelagic sediments (HS) are usually called upon to be involved in primary magmas of typical island Quaternary arc volcanics (e.g. Ishikawa and Nakamura, 1994). If the end member components of primary magma of SW Colombian arc is also mantle wedge, AOC and HS, the Pb isotopic compositions of the primary magmas of VF and RA in the studied region, should be within the triangle that consists of mantle wedge, AOC and HS, and plot in the mixing trend with the lower crust end-member. However, the intersections of VF and RA indicate that involvement of subduction component to RA magma is larger than that to the VF magma, which is in contrast with the relationship observed in typical island arcs (e.g. Izu and NE Japan arcs) where the involvement of subduction component to arc magma is decreased from VF toward RA, resulting that the Pb isotopic composition of primary magmas is more radiogenic in the VF compared to the RA (Ishikawa and Nakamura, 1994). Therefore, the unusual behaviour of the SW Colombian arc requires an additional Pb component for the formation of primary magmas at the volcanic front. We interpret to be the less-radiogenic carbonate-rich sediments (Fig. 7a) on the basis of the available Pb isotopic data from sediments of the Eastern Pacific Rise (DSDP site 495; Plank et al., 2002).

The effect of carbonates in the generation of the primary magmas is also clearly shown in the Hf–Pb and Hf–Nd isotope systematics (Fig. 7b and c), which is due to the contrasting isotopic characteristics of carbonate-rich sediments compared with the other subduction components (e.g. AOC and HS). The VF and the RA volcanic rocks lie on different εHf and Pb isotope trends (Fig. 7b). We also note two different trends in the εHf–εNd plot (Fig. 7c): (i) a horizontal array formed by the VF rocks, with almost constant εHf and variable εNd, indicating a larger influence of CS in the mantle source at the volcanic front compared to the rear arc and (ii) a mantle-terrigenous array in the RA volcanic rocks, controlled by mainly dehydration processes and less or negligible influence from fluids related to carbonate-rich sediments decarbonation. The higher Hf isotopic ratios at the VF volcanoes are consistent with the data shown for deep-sea marine sediments (Petke et al., 2002; Chauvel et al., 2008).

In summary, three end-members: AOC, HS and CS, are needed to produce the subduction component, which metasomatize the mantle wedge. We can assume that the mantle wedge beneath SW Colombian arc is similar in composition to a MORB-like mantle by the following reasons: (1) The available data of Sr and Nd isotope compositions of spinel peridotites xenoliths in SW Colombian rear arc indicate the presence of depleted mantle beneath the arc (Rodriguez-Vargas et al., 2005). (2) The compositional effect of Galapagos plume is confined to 450 km (Schilling et al., 1976; Pedersen and Furnes, 2001). Therefore, the influence of Galapagos plume to the SW Colombian arc located more than 450 km far from the spreading center is weak or negligible.

The notable correlation of SW Colombian samples and the lower continental crust (LCC) on the basis of LCC-xenoliths at this region (Weber et al., 2002) might reflect strong contributions of the underlying crust to the petrogenesis of the Quaternary lavas across-arc. Conventional Pb isotope plots indicate that all lavas are relatively radiogenic and are very similar to the LCC, which have basalt composition formed mainly by garnet-bearing amphibolites and pyroxenites, with conspicuous scapolite crystallization which may indicate the role of CO2-rich fluids metasomatism (Weber et al., 2002). Finally, once primary magmas are formed they may undergo a large degree of lower crus-

Table 2
Estimated isotopic compositions and parameters used for the mixing calculations curves.

End member	$^{208}Pb/^{204}Pb$	$^{206}Pb/^{204}Pb$	$^{176}Hf/^{177}Hf$	εHf	$^{143}Nd/^{144}Nd$	εNd	Pb (ppm)	Hf (ppm)	Nd (ppm)
AOC (1)	38.14	18.59	0.28297	7	0.512997	7	0.52	0.7	4.42
HS (2, 3, 4)	38.86	18.64	0.282738	−1.2	0.51247	−3.28	9.59	5	17.77
CS (2, 3, 4, 5)	38.16	18.46	0.283108	11.9	0.512415	−4.35	3.7	2	6.79
PM_VF[a]	38.1	18.49	0.283046	9.7	0.512459	−3.49	4.57	0.68	3.94
PM_RA[a]	38.3	18.59	0.282871	3.5	0.512745	2.09	4.69	3.67	30.68
M_wedge (6, 7)	37.9	18.5	0.28328	18	0.5131	10.87	0.02	0.15	0.71
LCC (8)	38.9	19.1	0.283026[b]	8.99[b]	0.51309	8.82	8.81	4.07	9.5

Dfluid at VF 4 GPa. 900 °C(9) Pb: 31.41; Nd: 1.51; Hf: 0.52.
Dfluid at RA 6 Gpa. 1000 °C (9) Pb: 43.63; Nd: 19.58; Hf: 5.26.

[a] Calculated values from graphic interpolation, concentrations of trace elements using Bathc equilibrium model for the mantle MORB type, assumed mantle composition: 5% cpx, 25% opx, 70% ol, using Kd values from Halliday et al., 1995.

[b] Hf data from the present study, sample $X = 11$. PM: primary magma; M_wedge: mantle wedge; LCC: lower continental crust. Refs: (1) Pedersen and Furnes, 2001; (2) Plank and Langmuir, 1998; (3) Patino et al., 2000; (4) Vervoort et al., 1999. (5) Hemming and McLeannan, 2001; (6) Salters and Stracke, 2004; (7) Saunders et al, 1988; (8) Weber et al., 2002; (9) Kessel et al., 2005.

tal assimilation, as it is supported by all the isotopic systematics. The assimilation of upper crust appears to be weak or negligible across-arc.

5.2. Mass-balance multi-isotopic aproach

We estimated the contents and isotopic ratios of Pb, Nd, Hf and Sr of each end-member component to form SW Colombian arc magmas (Table 2), based on available parameters such as partition coefficients between fluids and solid (D_{fluid}). The Pb isotopic composition of subduction components involved were constrained using Pb isotope diagrams (Fig. 7a); the proportions derived from the AOC and subducted sediments were assumed as 90% and 10%, respectively from Li, B, Pb, Sr and Nd isotope systematics studies in volcanic arcs (e.g. Ishikawa and Nakamura, 1994; Moriguti et al., 2004a,b). Then, the Nd and Hf isotope composition of the subduction components were interpolated graphically in the εNd–Pb and εNd–εHf isotopic systematics (Fig. 7b and c). Pb, Hf and Nd contents of slab-derived fluids were calculated using experimentally determined D_{fluid} derived from the MORB-fluid system (Kessel et al., 2005) (Table 2). Thus, the D_{fluid} by Kessel et al. (2005) can be used for the pressure and temperature condition of VF (4 GPa, 900 °C) and the RA (6 GPa, 1000 °C) in SW Colombian arc to model our data. These pressure and temperature conditions at the surface of the subducted slab beneath the VF and the RA were adopted from the estimated geotherms at relatively warm subduction zones (van Keken et al., 2002) using the age, 14–20 Ma (Hardy, 1991; Gutscher et al., 1999) and convergence rate, 6–7 cm/year (Gutscher et al., 1999) of the slab beneath the SW Colombian arc.

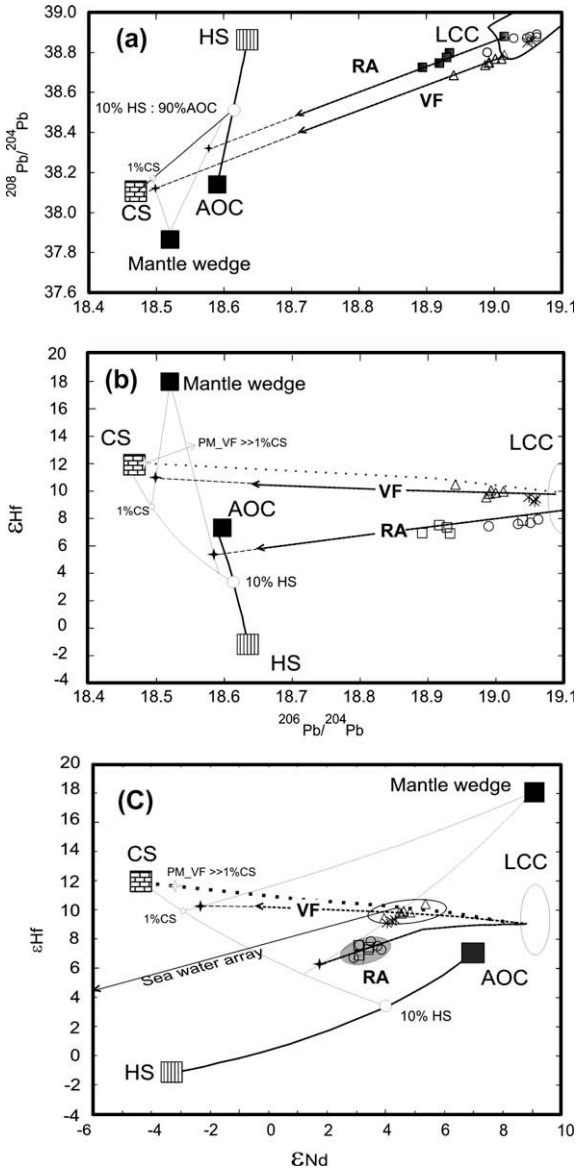

Fig. 7. (a–c) Schematic illustration of proposed model in (a) $^{208}Pb/^{204}Pb$ vs. $^{206}Pb/^{204}Pb$; (b) εHf vs. $^{206}Pb/^{204}Pb$; (c) εHf vs. εNd for the SW Colombian volcanic arc (d) Sr–Nd isotopic systematics. Symbols of each volcano are the same as those in Fig. 3. Stars symbols represent the calculated primary magma at the VF (solid star) and the RA (gray star). Multiple isotopic systematics clearly shows the contribution of the following end-members to the volcanic front magmas: altered oceanic crust (AOC), hemipelagic sediments (HS), carbonate-rich sediments (CS), wedge mantle (MORB-like) and lower continental crust (LCC). Data from Table 2.

In the mass balance calculation, to estimate CS component in the subduction component added to the primary magma quantitatively, representative data of Pb, Nd and Hf content and the isotope ratios of each end member component (CS, AOC, HS, mantle wedge and LCC) were used following the references cited in Table 2 and the range of variation of their isotopic compositions are shown in Fig. 7a–c. The results of mass-balance calculations in Pb, Nd and Hf isotope systematics data, indicate that at least ~1% of CS component was involved into subduction component in the magma of SW Colombian arc (see Fig. 7a–c). On the other hand, the involvement of the carbonate sediments in the subduction component at the RA is insignificant.

It has been suggested that the aqueous fluids liberated from subducted slab are decreasingly added to the depleted mantle across-arc with increasing depth to WBZ. This might result in different degrees of partial melting at the VF compared to the RA (e.g. Ishikawa and Nakamura, 1994; Rüpke et al., 2002). The across-arc variation of Ba/Nb, Ba/Th and Pb/Ce in SW Colombian arc may reflect this decrease of amount of aqueous fluids from slab. If this is the case, the aqueous fluids could control the decrease of carbonate component in the subduction components from VF to RA, resulting in a difference in the isotopic compositions of the primary magmas with the depth of WBZ, which has relatively high Hf isotopic ratio and low Pb isotopic ratio at VF compared to the RA (see Table 2).

The above-mentioned end-member components of the magmas of studied samples are well distinguished in the Sr and Nd isotopic systematics (Fig. 8). In order to draw the mixing curves, the following assumptions were: (1) Subduction components consist of CS with HS and AOC (HS/AOC = 10/90); (2) εNd values of subduction components at VF and RA are −2.9 and 1.2, respectively, obtained from Hf and Nd isotope systematics (Fig. 7c).

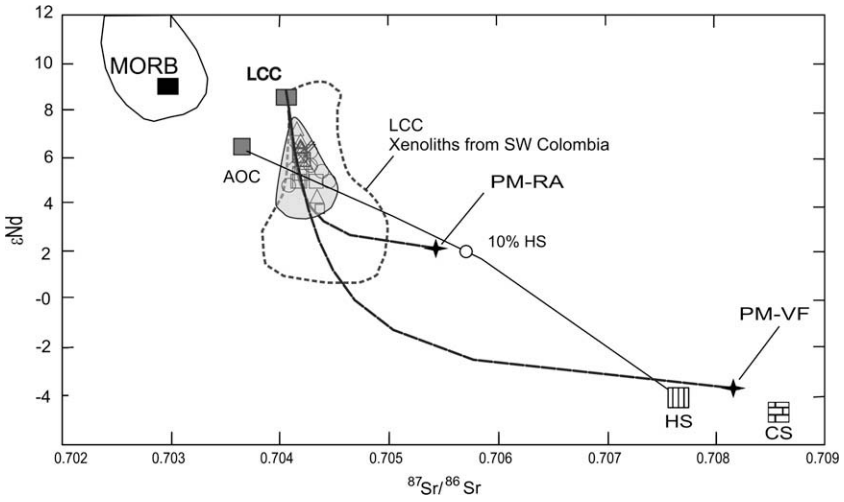

Fig. 8. Sr-Nd isotopic systematics for the SW Colombian Quaternary lavas. Stars represent the primary magma isotopic composition for the mantle-derived magmas modified by the subduction component at VF and RA following the similar approaches in the Fig. 7. Fields in the Sr–Nd diagram are from: Colombian volcanoes (present study); LCC xenoliths, from Weber et al. (2002). Atlantic and Pacific MORB (Cohen and O'Nions, 1982. White and Hofmann, 1982; Ito et al., 1987). Hemipelagic sediments (HS) and Carbonate rich sediments (CS) from Patiño et al. (2000) and Plank and Langmuir (1998).

As shown in Fig. 8, primary magma compositions of VF and RA are discriminated from each other clearly. However, mixing curves between primary magmas and LCC for VF lavas and RA lavas come close to each other near LCC area. Therefore, involvement of LCC would cause restricted Sr isotopic composition of studies samples (0.704167–0.704461). The resulting Sr isotope systematics in this arc volcanics is not helpful in the evaluation of the extent of contribution of CS to primary magma. Rather, the Hf and Pb isotope systematics and the Pb isotope plots are the most useful in pointing to the differences between the VF an RA volcanic suites, with more involvement of CS in the VF compared to the RA. Thus, it appears that Pb signatures either related to efficient retention of end-members Pb signature during slab-metamorphism or faithful transfer or the fractionated Pb signature by metamorphic fluid flow, may indicate the effect of melange mixing in the subduction-zone mass transfer as has been pointed out in studies of high-pressure and ultra-high pressure metamorphic suites (King et al., 2007).

An open question remains as to the involvement of carbonates in the arc magmas: If significant CO_2 liberation takes place at sub-arc depths then CO_2 might influence the major element composition of the primary magmas especially at the volcanic front, and produce silica-undersaturated magmas. However, it is still difficult to evaluate the effect of the liberated CO_2 to the major element composition of arc magmas in this region, because the erupted andesites have been strongly contaminated by assimilation of Pb-radiogenic lower crust (up to 20%, see Fig. 8a–c and Fig. 8), which may control the major element composition of arc lavas and may erase the effect of CO_2 liberated from subducted slab to primary magmas at major element level, but it remains as a clear signature in their isotopic composition such as the mixing trends in the Pb isotopes.

5.3. Roles of aqueous fluids in decarbonation at subduction zones and carbon recycling

The results of high-pressure experiments indicate that carbonates are stable in eclogite residue under subduction zone P–T condition (Yaxley et al., 1994; Dasgupta et al., 2004; Yaxley and Brey, 2004; Thomsen and Schmidt, 2008). However, influx of hydrous fluids likely will affect decarbonation reactions (e.g. Molina and Poli, 2000; Gorman et al., 2006). In addition, aqueous fluids from the subducted slab can induce CO_2 liberation into the fluid due to the replacement of carbonates during the eclogitization processes occurring in the AOC (see John et al., 2008). Therefore, slab decarbonation at sub-arc is inevitably linked to dehydration. The question is whether dehydration and decarbonation occur simultaneously in space and time (i.e., batch models) or whether infiltration of water released at depth triggers shallower decarbonation. Even in the case of young subduction Nazca plate beneath SW Colombian arc there is no particular problem in explaining the inferred decarbonation by either mechanism. However, it seems that the detection of a clear carbonate sediment (CS) isotopic signal is at odds with the infiltration-driven decarbonation mechanism. If we assume large amounts of water derived by deserpentinization at depth, this signal could be obliterated. Thus the fact that we can explain the formation of the primary magmas by the addition of three subducted components (CS, HS and AOC) may support a batch devolatilization model and incidentally suggests that the mantle is not heavily serpentinized in this region.

Our findings of carbonate involvement at volcanic front volcanoes is consistent with the results from C and N isotopic studies of fumarolic gases from the Galeras volcanic complex (Fischer et al., 1997) located at the volcanic front in the SW Colombian arc. At the volcanic front in the Central American Volcanic Arc, similar signature of carbonate

involvement has been also observed (e.g. Patiño et al., 2000; Plank et al., 2002, Shaw et al., 2003; Leeuw et al., 2007). In those areas, limestone and/or marine carbonate sediments can also be subducted.

The presence of more aqueous fluids at the VF could enhance the degree of decarbonation in the slab. The infiltration of H_2O-rich fluids derived from the AOC into carbonate-bearing lithologies in equilibrium with a H_2O-rich and CO_2 poor fluid mixture reduces the activity of CO_2 by dilution, thus inducing metamorphic decarbonation (Ferry, 1991). Moreover, taking into account recent thermal models at subduction zones (van Keken et al., 2002), which are hotter than the previous models (e.g. Peacock and Wang, 1999), several types of decarbonation reactions in subducted GLOSS average marine sediments, siliceous limestone and carbonate oozes modelled by Kerrick and Connolly (1998) may play an important role in supplying CO_2 to the volcanic front volcanoes in almost all thermal regimes induced by aqueous fluids.

The multi-isotopic approach in the natural samples of the SW Colombian arc, allow us to trace the involvement of carbonate-rich sediments in arc magmas, which indicates that decarbonation can occur at the sub-arc region but the extent of decarbonation can be reduced with the depth of WBZ. Additionally, the successive decrease of Ba/Nb ratios from VF to RA (Fig. 6) indicates that the contribution of aqueous components from slab to arc magmas decreases with the depth of WBZ because the solubility of Ba is significantly higher (e.g. Gill, 1981) than that of Nb and the incompatibility of Ba is similar to that of Nb. We conclude, therefore, that carbonate-rich sediments experiences continuous decarbonation induced by dehydration during subduction at sub arc region and these decarbonation processes are mainly controlled by the amount of aqueous fluids released from continuous slab dehydration. However, the increasing pressure and temperature in the subduction system ultimately leads to the cessation of fluid-induced decarbonation reactions at the rear arc. This may allow the remaining carbonate materials (carbonate eclogite) to proceed to higher pressures as has also been proposed elsewhere (Yaxley and Green, 1994; Molina and Poli, 2000; Dasgupta et al., 2004; Yaxley and Brey, 2004). Experimental results at upper mantle pressure-temperature conditions indicate that subducted carbonate eclogite can melt at depths near 300–400 km, leading to the formation of carbonatites (Dasgupta et al., 2004; Yaxley and Brey, 2004).

Our hypothesis can be supported on the fact that the stability of carbonate-rich lithologies at subduction zones is highly dependent on pressure, temperature, CO_2 activity in the ambient fluid, oxygen fugacity and bulk composition (e.g. Will et al., 1990; Yaxley and Green, 1994). Recent studies in the subducted oceanic crust showed that the heterogeneous oxidation of the subducting lithosphere can control the potential for the production of C·O·H fluid mixtures, which induces the production of distinct fluid populations (e.g. Poli et al., 2009), resulting in the formation of different isotopic primary magmas across-arc.

6. CONCLUSIONS

We can conclude that subducted slab can introduce some carbonate materials to significant mantle depths in most subduction zones. Our results also show that for the SW Colombian arc, the fluid from the subduction component (AOC + HS + CS) should be added to the mantle wedge up to the depths of ~200 km of the WBZ where the last volcano in the rear arc is located (Fig. 9). Moreover,

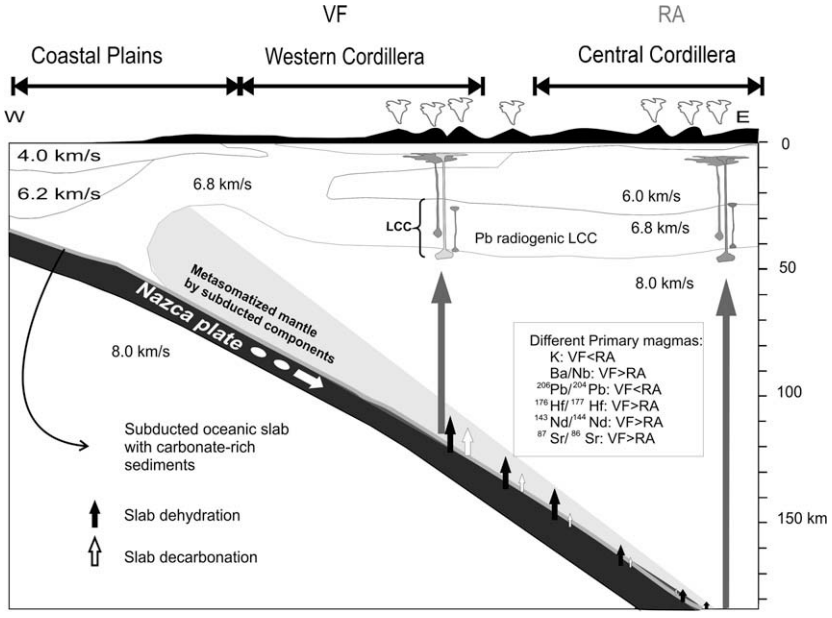

Fig. 9. Modified geophysical cross-section of SW Colombian arc inferred from seismological data by Meissner et al. (1976) and a general model for the interaction between subducted oceanic slab and wedge mantle and the formation of SW Colombian andesites by assimilation of lower continental crust materials.

the isotope systematics indicate that carbonates contribute to arc volcanoes in varying proportions (~1% involvement) at the volcanic front and becoming negligible at depths >200 km, due to the progressive cessation of fluid/induced decarbonation reactions with the diminishing of slab dehydration. Consequently, the remaining subducted carbonates appear likely to be recycled and serve as a carrier of carbon to the deep mantle. This implies that transportation processes of carbon from sediments in the oceans to the atmosphere through active volcanic arcs are not efficient.

In rigorous estimation of CO_2-fluxes at subduction zones, however, it is necessary to take into account variations in the proportion of CO_2 carried by aqueous fluids transferred from the slab to the mantle wedge as a function of depth to the WBZ.

Finally, one of the most important implications of this study in the deep carbon-cycle is that even if some amount of carbonate-rich sediments are removed at the fore-arc and sub-arc regions, carbonate-rich sediments can potentially deliver carbon to the mantle via subducted carbonate eclogite. If the subducted slab is recycled into the sources of ocean-island basalts (OIB), the presence of residual carbonate which have a relatively high $^{176}Hf/^{177}Hf$ ratio may also be recycled (Chauvel et al., 2008) and it may explain the isotopic signatures found in some Hawaiian basalts (Blichert-Toft et al., 1999) and may contribute to the C-fluxes estimated for OIB (Marty and Tolstikhin, 1998).

ACKNOWLEDGMENTS

We thank T. Tsujimori, R. Tanaka, K. Kobayashi I. Campbell, M. Feineman, and B. Paul, for constructive reviews of this manuscript. Special thanks to the PML staff: K. Yamashita and C. Sakaguchi for their scientific guidance, technical support and valuable discussion. We also want to thanks the Associate editor B. Mysen, and the reviewers S. Poli, G. Bebout and the anonymous reviewer for their suggestions, which highly improved the quality of the present manuscript. This study was financially supported by the program "Center of Excellence for the 21st Century in Japan" (E.N.) and in part by grants from the Ministry of Education, Science, Sports and Culture of Japan (T.M).

REFERENCES

Alvarado G. E., Denyer P. and Sinton C. W. (1997) The 89 Ma Tortugal komatiitic suite, Costa Rica: implications for a common geological origin of the Caribbean and Eastern Pacific region from a mantle plume. *Geology* **25**, 439–442.

Arango J. L. and Ponce A. (1982) Mapa Geológico del Departamento de Nariño, escala 1: 400,000. *Memoria Explicativa Ingeominas* **18**, 1–88.

Arculus R. J., Lapierre H. and Jaillard E. (1999) Geochemical window into subduction and accretion processes: Raspas Metamorphic Complex, Ecuador. *Geology* **27**, 547–550.

Barret T. J., Taylor P. N. and Lugowski J. (1987) Metalliferous sediments from DSDP leg 92: the East Pacific Rise transects. *Geochim. Cosmochim. Acta* **46**, 651–666.

Bechon F., Monsalve M.L. (1991) Activité récernte phéhistorique du volcan Azufral (S-W de la Colombie). *C.R. Acad. Sci. Paris, t.* **313**(Série II), 99–104.

Blichert-Toft J., Frey F. A. and Albarede F. (1999) Hf isotope evidence for pelagic sediments in the Source of Hawaiian Basalts. *Science* **285**, 879–882.

Calvache M. L. and Williams S. (1997) Geochemistry and Petrology of the Galeras volcanic complex, Colombia. *J. Volcanol. Geo. Res.*, 7721–7738.

Connolly J. A. (2005) Computation of phase equilibria by linear programming: a tool for geodynamic modelling and its application to subduction zone decarbonation. *Earth Planet. Sci. Lett.* **236**, 524–541.

Cohen R. S. and O'Nions R. K. (1982) The lead, neodymium and strontium isotopic structure of Ocean Ridge basalts. *J. Petrol.* **23**, 299–324.

Chauvel C., Lewin E., Carpentier M., Arndt N. T. and Marini J.-C. (2008) Role of recycled oceanic basalt and sediment in generating the Hf–Nd mantle array. *Nat. Geosci.* **1**, 64–67.

Chiaradia M. and Fontbote L. (2002) Lead isotope systematics of Late Cretaceous–Tertiary Andean arc magmas and associated ores between 8 N and 40 S: evidence for latitudinal mantle heterogeneity beneath the Andes. *Terra Nova* **14**(5), 337–342.

Dasgupta R., Hirschmann M. M. and Withers A. C. (2004) Deep global cycling of carbon constrained by the solidus of anhydrous, carbonated eclogite under upper mantle conditions. *Earth Planet. Sci. Lett.* **227**, 73–85.

Dasch E. J. (1981) Lead isotopic composition of metalliferous sediments from the Nazca plate. *Geol. Soc. Am. Mem.* **154**, 199–200.

Defant M. J. and Drummond M. S. (1990) Derivation of some modern arc magmas by melting of young subducted lithosphere. *Nature* **347**, 662–665.

Droux A. and Delaloye M. (1996) Petrography and geochemistry of Plio-Quaternary Calc-Alkaline Volcanoes of Southwestern Colombia. *J. S. Am. Earth Sci.* **9**, 27–41.

Edmond J. and Huh Y. (2003) Non-steady state carbonate recycling and implications for the evolution of atmospheric pCO_2. *Earth Planet. Sci. Lett.* **216**, 125–139.

Ferry J. M. (1991) Dehydration and decarbonation reactions as a record for fluid infiltration. *Rev. Mineral. Geochem.* **26**(1), 351–393.

Fischer T., Sturchio N., Stix J. and Arehart G. (1997) The chemical and isotopic composition of fumarolic gases and spring discharges form Galeras Volcano. *Colombia. J. Volcanol. Geo. Res.* **77**, 229–253.

Gill J. B. (1981) *Orogenic Andesites and Plate Tectonics*. Springer, Heidelberg.

Gorman P. J., Kerrick D. M. and Connolly J. A. D. (2006) Modelling open system metamorphic decarbonation of subducting slabs. *Geochem. Geophys. Geosys.* **7**(4), Q04007. doi:10.1029/2005GC001125.

Gutscher M. A., Malavieille J., Lallemand S. and Collot J. Y. (1999) Tectonic segmentation of the North Andean margin: impact of the Carnegie Ridge collision. *Earth Planet. Sci. Lett.* **168**, 255–270.

Hardy N. C. (1991) Tectonic evolution of the easternmost Panama Basin: some new data and interferences. *J. S. Am. Earth Sci.* **4**(3), 261–269.

Harmon R. S., Barreiro B., Moorbath S., Hoefs J., Francis P. W., Thorpe R. S., Deruelle B., McHugh J. and Viglino J. A. (1984) Regional O-, Sr-, and Pb-isotope relationships in late Cenozoic calc-alkaline lavas of the Andean Cordillera. *J. Geol. Soc.* **141**(5), 803–822.

Hawkesworth C. and Clarke C. (1994) Partial melting in the lower crust: new constraints on crustal contamination processes in the Central Andes. In *Tectonics of the Southern Central Andes, Structure and Evolution of an Active Continental Margin* (eds. K.

J. Reutter, E. Scheuber and P. J. Wigger). Springer Verlag, Berlin, pp. 93–101.

Hemming S. R. and McLeannan (2001) Pb isotopic compositions of modern deep seaturbidites. *Earth Planet. Sci. Lett.* **184**, 489–503.

Hildreth W. and Moorbath S. (1988) Crustal contribution to arc magmatism in the Andes of central Chile. *Contrib. Mineral. Petrol.* **98**, 455–489.

Hochstaedter A., Gill J., Peters R., Broughton P., Holden P. and Taylor B. (2001) Across-arc geochemical trends in the Izu-Bonin arc: contributions from the subducting slab. *Geochem. Geophys. Geosyst.* **2**, 2000GC000105.

Ishikawa T. and Nakamura E. (1994) Origin of the slab component in arc lavas from across-arc variation of B and Pb isotopes. *Nature* **370**, 205–208.

Ishikawa T. and Tera F. (1997) Composition and distribution of the fluid in the Kurile mantle wedge: constraints from across-arc variations of B/Nb and B isotopes. *Earth Planet. Sci. Lett.* **152**, 123–138.

Ishikawa T., Tera F. and Nakazawa T. (2001) Boron isotope and trace element systematics of the three volcanic zones in the Kamchatka arc. *Geochim. Cosmochim. Acta* **63**, 3337–3347.

Ito E., White W. M. and Göpel C. (1987) The O, Sr, Nd, and Pb isotope geochemistry of MORB. *Chem. Geol.* **62**, 157–176.

John T., Klemd R., Gao J. and Garbe-Schönberg C. (2008) Trace-element mobilization in slabs due to non steady-stare fluid-rock interaction: constraints from an eclogite-facies transport vein in blueschist (Tianshan, China). *Lithos* **103**. doi:10.1016/j.lithos.2007.09.005, pp. 1–2, 1–24.

Kerr A. C., Marriner G. F., Arndt N. T., Tarney J., Nivia A., Saunders A. D. and Duncan R. A. (1996) The petrogenesis of Gorgona komatiites, picrites and basalts: new field, petrographic and geoÙchemical constraints. *Lithos* **37**, 245–260.

Kerrick D. M. and Connolly J. A. D. (1998) Subduction of ophicarbonates and recycling of CO_2 and H_2O. *Geology* **26**, 375–378.

Kerrick D. M. and Connolly J. A. D. (2001a) Metamorphic devolatilization of subducted marine sediments and transport of volatiles into the Earth's mantle. *Nature* **411**, 293–296.

Kerrick D. M. and Connolly J. A. D. (2001b) Metamorphic devolatilization of subducted oceanic metabasalts: implications for seismicity, arc magmatism and volatile recycling. *Earth Planet. Sci. Lett.* **189**, 19–29.

Kennedy C. S. and Kennedy G. C. (1976) The equilibrium boundary between graphite and diamond. *J. Geophys. Res.* **81**, 2467–2470.

Kessel R., Schmidt M. W., Ulmer P. and Pettke T. (2005) Trace element signature of subduction-zone fluids, melts and supercritical liquids at 120–180 km depth. *Nature* **437**, 724–727, doi:710.1038/nature03971.

King R. L., Bebout G. E., Grove M., Moriguti T. and Nakamura E. (2007) Boron and lead isotope signatures of subduction-zone mélange formation: hybridization and fractionation along the slab–mantle interface beneath volcanic arcs. *Chem. Geol.* **239**(3–4), 305–322.

Kuritani T. and Nakamura E. (2003) Highly precise and accurate isotopic analysis of small amounts of Pb using 205Pb–204Pb and 207Pb–204Pb, two double spikes. *J. Anal. At. Spectrom.* **18**, 1464–1470.

LeMaitre R. W., Bateman P., Dudek A., Keller J., Lameyre-LeBas M. J., Sabine P. A., Schmid R., Sorensen H., Streckeisen A., Woolley A. R. and Zanettin B. A. (1989) *Classification of Igneous Rocks and Glossary of Terms*. Blackwell, Oxford.

Leeuw G. A. M., Hilton D. R., Fischer T. P. and Walker J. A. (2007) The He–CO_2 isotope and relative abundance characteristics of geothermal fluids in El Salvador and Honduras: new constraints on volatile mass balance of the Central American Volcanic Arc. *Earth Planet. Sci. Lett.* **258**(1–2), 132–146.

Lu Y.-H., Makishima A. and Nakamura E. (2007) Purification of Hf in silicate materials using extraction chromatographic resin, and its application to precise determination of $^{176}Hf/^{177}Hf$ by MC-ICP-MS with 179Hf spike. *J. Anal. At. Spectrom.* **22**, 69–76.

McDonough W. F. and Sun S.-S. (1995) Composition of the Earth. *Chem. Geol.* **120**, 223–253. doi:10.1016/0009-2541(94)00140-4.

Makishima A. and Nakamura E. (2006) Determination of major, minor and trace elements in silicate samples by ICP-QMS and ICP-SFMS applying isotope dilution-internal standardization (ID-IS) and multi-stage internal standardization. *Geostand. Geoanal. Res.* **30**, 245–271.

Makishima A., Nath B. N. and Nakamura E. (2008) New sequential separation procedure for Sr, Nd and Pb isotope ratio measurement in geological material using MC-ICP-MS and TIMS. *Geochem. J.* **42**, 237–246.

Makishima A., Nakamura E. and Nakano T. (1999) Determination of zirconium, niobium, hafnium and tantalum at ng/g levels in geological materials by direct nebulization of samples HF solution into FI-ICP-MS. *Geostand. Newslet.* **23**, 7–20.

Mamberti M., Hernandez J., Lapierre H., Bosch D., Jaillard E., Ethien R. and Polvé M. (2003) Accreted fragments of the Late Cretaceous Caribbean–Colombian Plateau in Ecuador. *Lithos* **173**, 199.

Marin-Cerón M.I. (2002) Informe final de la componente geoesférica in: Proyecto Complejo Volcánico Doña Juana – Cerro Juanoy. *IDEAM,* 019077.MG. Bogotá – Colombia. Available from: <http://torcard.ideam.gov.co/cgi-bin/ideam.pl>.

Marini J.-C., Chauvel C. and Maury R. (2005) Hf isotope compositions of northern Luzon arc lavas suggest involvement of pelagic sediments in their source. *Contrib. Mineral. Petrol.* **149**, 216–232, doi:101007/s00410-004-0645-4.

Marty B. and Tolstikhin I. (1998) CO_2 fluxes from mid-ocean ridges, arcs and plumes. *Chem. Geol.* **145**, 233–248.

Meissner R. O., Flueh E. R., Stibane F. and Berg E. (1976) Dynamics of the active plate boundary in southwest Colombia according to recent geophysical measurements. *Tectonophysics* **35**, 115–136.

Molina J. F. and Poli S. (2000) Carbonate stability and fluid composition in subducted oceanic crust: an experimental study on H_2O–CO_2-bearing basalts. *Earth Planet. Sci. Lett.* **176**, 295–310.

Morlidge M., Pawley A. and Giles D. (2006) Double carbonates breakdown reactions at high pressures: an experimental study in the system CaO–MgO–FeO–MnO–CO_2. *Contrib. Mineral. Petrol.* **152**, 365–373.

Moriguti T., Shibata T. and Nakamura E. (2004a) Lithium, boron and lead isotope and trace element systematics of Quaternary basaltic volcanic rocks in northeastern Japan: mineralogical controls on slab-derived fluid composition. *Chem. Geol.* **212**, 81–100.

Moriguti T., Makishima A. and Nakamura E. (2004b) Determination for lithium contents in silicates by isotope dilution ICP-MS and its evaluation by isotope dilution TIMS. *Geostand. Newslet.* **28**, 371–382.

Morris D. and Tera F. (1989) ^{10}Be and ^{9}Be in mineral separates and whole rocks from volcanic arcs: implications for sediment subduction. *Geochim. Cosmochim. Acta* **53**, 3197–3206.

Murcia A. and Marin P. (1980) *Petrología y Petroquímica en Lavas Recientes de Algunos Volcanes en Colombia*. I Seminario sobre el Cuaternario de Colombia, Bogota, 30.

Nakamura E., Campbell I. H. and Sun S. S. (1985) The influence of subduction processes on the geochemistry of Japanese alkaline basalt. *Nature* **316**, 55–58.

Nakamura E., Makishima A., Moriguti T., Kobayashi K., Sakaguchi C., Yokoyama T., Tanaka R., Kuritani T. and Takei H. (2003) Comprehensive geochemical analyses of small amounts (< 100 mg) of extraterrestrial samples for the analytical competition related to the sample return mission MUSES-C. *Inst. Space Astronaut. Sci. Rep. SP.* **16**, 49–101.

Nowell G. M., Kempton P. D., Noble S. R., Fitton J. G., Saunders A. D., Mahoney J. J. and Taylor R. N. (1998) High precision Hf isotope measurements of MORB and OIB by thermal ionisation mass spectrometry: insights into the depleted mantle. *Chem. Geol.* **149**, 211–233.

Patiño L. C., Carr M. and Feigenson M. (2000) Local and regional variations in Central American arc lavas controlled by variations in subducted sediment input. *Contrib. Mineral. Petrol.* **138**, 265–283.

Peacock S. M. and Wang K. (1999) Seismic consequences of warm versus cool subduction metamorphism: examples from Southwest and Northeast Japan. *Science* **286**, 937–939.

Pearce J. A., Kempoton P. D., Nowell G. M. and Noble S. R. (1999) Hf–Nd Element and isotope perspective on the nature and provenance of mantle and subduction components in Westen Pacific arc-Basin systems. *J. Petrol.* **40**(11), 1579–1611.

Pedersen R. and Furnes H. (2001) Nd- and Pb-isotopic variations through the upper oceanic crust in DSDP/ODP Hole 504B, Costa Rica Rift. *Earth Planet. Sci. Lett.* **189**, 221–235.

Perfit M. R., Gust A. E., Bence A. E., Arculus R. J. and Taylor S. R. (1979) Chemical characteristics of island-arc basalts: implications for mantle sources. *Chem. Geol.* **30**, 227–256.

Petke T., Lee D. C., Halliday A. N. and Rea D. K. (2002) Radiogenic Hf isotopic compositions of continental eolian dust from Asia, its variability and its implications for seawater Hf. *Earth Planet. Sci. Lett.* **202**, 453–463.

Plank T. and Langmuir C. (1998) The chemical composition of subducting sediment and its consequences for the crust and mantle. *Chem. Geol.* **145**, 325–394.

Plank T., Balzer V. and Carr M. (2002) Nicaraguan volcanoes record paleoceanographic changes accompanying closure of the Panama gateway. *Geology* **30**, 1087–1090.

Poli S., Franzolin E., Fumagalli P. and Crottini A. (2009) The transport of carbon and hydrogen in subducted oceanic crust: an experimental study to 5 GPa. *Earth Planet. Sci. Lett.* **278**(3–4), 350–360.

Pulgarin B., Monsalve M. L., Arcila M. and Cepeda H. (1993) Actividad histórica y actual del volcán Puracé, Colombia. *Bol. Geol. Ingeominas* **34**, 39–53.

Rodriguez-Vargas A., Koester E., Mallmann G., Conceicao R. V., Kawashita K. and Weber M. B. I. (2005) Mantle diversity beneath the Colombian Andes, Northern Volcanic Zone: constraints from Sr and Nd isotopes. *Lithos* **82**, 471–484.

Rüpke L., Morgan J., Hort M. and Connolly J. (2002) Are the regional variations in Central arc lavas due to differing basaltic versus peridotitic slab sources of fluids? *Geology* **30**, 1035–1038.

Ryan J. and Langmuir C. (1987) The systematics of lithium abundances in young volcanic rocks. *Geoch. Cosm. Acta.* **51**, 1727–1741.

Sadofsky S. and Bebout G. (2003) Record of forearc devolatilization in low-T, high-P/T metasedimentary suites: significance for models of convergent margin chemical cycling. *Geochem. Geophys. Geosys.* **4**(4). doi:10.1029/2002GC000412.

Sakuyama M. and Nesbrit R. W. (1986) Geochemistry of the Quaternary volcanic rocks of the Northeast Japan arc. *J. Volcanol. Geo. Res.* **29**, 413–450.

Salters V. and Stracke A. (2004) Composition of depleted mantle. *Geochem. Geophys. Geosys.* **5**(5). doi:10.1029/ 2003GC000597.

Sano Y. and Williams S. N. (1996) Fluxes of mantle and subducted carbon along convergent plate boundaries. *Geophys. Res. Lett.* **23**, 2749–2752.

Sato K. and Katsura T. (2001) Experimental investigation on dolomite dissociation into aragonite + magnesite up to 8.5 GPa. *Earth. Planet. Sci. Lett.* **184**, 529–534.

Saunders A. D., Norry M. J. and Tarney J. (1988) Origin of MORB and chemically depleted mantle reservoirs: trace element constraints. *J. Petrol. Special Lithos. Issue* **1**, 415–445.

Shaw A. M., Hilton D. R., Fischer T. P., Walker J. A. and Alvarado G. E. (2003) Contrasting He–C relationships in Nicaragua and Costa Rica: insights into C cycling through subduction zones. *Earth. Planet. Sci. Lett.* **214**(3–4), 499–513.

Schilling J.-G., Anderson R. N. and Vogt P. (1976) Rare earth, Fe and Ti variations along the Galapagos spreading centre, and their relationship to the Galapagos mantle plume. *Nature* **261**, 108–113.

Snyder G., Poreda R., Hunt A. and Fehn U. (2001) Regional variations in volatile composition: Isotope evidence for carbonate recycling in the Central American volcanic arc. *Geochem. Geophys. Geosyst.* **2**(10). doi:10.1029/2001GC000163.

Takei H., Yokoyama T., Makishima A. and Nakamura E. (2001) Formation and suppression of AlF_3dufing HF digestion of tock samples in Teflon bomb for precise trace element analyses by ICP-MS and ID-TIMS. *Proc. Jpn. Acad.* **77**, 13–17.

Takei H. (2002) Development of precise analytical techniques for major and trace element concentrations in rock samples and their applications to the Hirashikari Gold Mine, southern Kyushu, Japan. *Doctoral thesis, Okayama Univ.*, **1**, 164 pp.

Thompson P. M., Kempton P. D., White V., Saunders A. D., Kerr A. C., Tarney J. and Pringle M. S. (2004) Elemental, Hf–Nd isotopic and geochronological constraints on an island arc sequence associated with the Cretaceous Caribbean plateau: Bonaire, Dutch Antilles. *Lithos* **74**, 91–116.

Thomsen T. B. and Schmidt M. W. (2008) Melting of carbonaceous pelites at 2.5–5.0 GPa, silicate–carbonatitie liquid immiscibility, and potassium–carbon metasomatism of the mantle. *Earth Planet. Sci. Lett.* **267**, 17–31.

Thorpe R. S. (1984) The tectonic setting of active Andean volcanism. In *Andean magmatism: Chemical and Isotopic Constraints* (eds. R. S. Harmon and B. A. Barreiro). Shiva Geological Series, Shiva Publications, Nantwich, UK, pp. 4–8.

van Keken P. E., Kiefer B. and Peacock S. M. (2002) High-resolution models of subduction zones: Implications for mineral dehydration reactions and the transport of water into the deep mantle. *Geochem. Geophys. Geosys.* **3**(10), 1056. doi:10.1029/2001GC000256.

Vervoort J., Patchett J., Blichert-Tofl J. and Albarede F. (1999) Relationships between Lu–Hf and Sm–Nd isotopic systematics in the global sedimentary system. *Earth Planet. Sci. Lett.* **168**, 79–99.

Weber M. B., Tarney J., Kempton P. D. and Kent R. W. (2002) Crustal make-up of the northern Andes: evidence based on deep crustal xenolith suites, Mercaderes, SW Colombia. *Tectonophysics* **345**, 49–82.

White W. M. and Hofmann A. W. (1982) Sr and Nd isotope geochemistry of oceanic basalts and mantle evolution. *Nature* **296**, 821–825, doi:10.1038/296821a0.

White W. M., Hofmann A. W. and Puchelt H. (1987) Isotope geochemistry of Pacific mid-ocean ridge basalts. *J. Geophys. Res.* **92**, 4881–4893.

White W. M., Patchett J. and Benothman D. (1986) Hf isotope ratios of marine sediments and Mn nodules: evidence for a mantle source of Hf in seawater. *Earth Planet. Sci. Lett.* **79**, 46–54.

Will T. M., Powell R., Holland T. and Guiraud M. (1990) Calculated green schistfacies mineral equilibria in the system $CaO–FeO–MgO–Al_2O_3–SiO_2–CO_2–H_2O$. *Contrib. Mineral. Petrol.* **104**, 353–368.

Wilson M. (1989) *Igneous Petrogenesis*. Chapman and Hall, London, UK, 457pp.

Yaxley G. M. and Brey G. P. (2004) Phase relations of carbonate-bearing eclogite assemblages from 2.5 to 5.5 GPa: implications for petrogenesis of carbonatites. *Contrib. Miner. Petrol.* **146**, 606–619.

Yaxley G. M. and Green D. H. (1994) Experimental demonstration of refractory carbonate-bearing eclogite and siliceous melt in the subduction regime. *Earth Planet. Sci. Lett.* **128**, 313–325.

Yaxley G. M., Green D. H. and Klapova H. (1994) The refractory nature of carbonate during partial melting of eclogite: evidence from high pressure experiments and natural carbonate-bearing eclogites. *Mineral. Mag.* **58A**, 996–997.

Yoshikawa M. and Nakamura E. (1993) Precise isotope determination of trace amounts of Sr in magnesium-rich samples, Japan. *J. Min. Pet. Econ. Geol.* **88**, 548–561.

Associate editor: Bjorn Mysen